

Array Gain for Pinching-Antenna Systems (PASS)

Chongjun Ouyang, Zhaolin Wang, Yuanwei Liu, *Fellow, IEEE*, and Zhiguo Ding, *Fellow, IEEE*

Abstract—Pinching antennas is a novel flexible-antenna technology, which can be realized by employing small dielectric particles on a waveguide. The aim of this letter is to characterize the array gain achieved by pinching-antenna systems (PASS). A closed-form upper bound on the array gain is derived by fixing the inter-antenna spacing. Asymptotic analyses of this bound are conducted by considering an infinitely large number of antennas, demonstrating the existence of an optimal number of antennas that maximizes the array gain. The relationship between the array gain and inter-antenna spacing is further explored by incorporating the effect of mutual coupling. It is proven that there also exists an optimal inter-antenna spacing that maximizes the array gain. Numerical results demonstrate that by optimizing the number of antennas and inter-antenna spacing, PASS can achieve a significantly larger array gain than conventional fixed-location antenna systems.

Index Terms—Array gain, mutual coupling, near-field communications, pinching-antenna systems (PASS).

I. INTRODUCTION

Recently, flexible-antenna systems, such as fluid antennas [1] and movable antennas [2], have gained significant research attention. In particular, these novel antenna types and array architectures can reconfigure wireless channel conditions by adjusting the positions of antennas and improve system performance. However, existing flexible-antenna systems face certain limitations. Specifically, antenna movements are often constrained within an aperture on an order of several wavelengths, which makes them ineffective at mitigating the impact of large-scale path loss. Additionally, many flexible-antenna systems are expensive to build, and their flexibility in reconfiguring the array architecture (e.g., adding or removing antennas) is limited.

To address these challenges, the pinching antenna has been proposed as a novel flexible-antenna technology [3], [4]. Utilizing a dielectric waveguide as a transmission medium, antennas in a pinching-antenna system (PASS) can be dynamically activated at any point along the waveguide, much like adding or releasing a clothespin to a clothesline [3], [4]. This yields highly flexible antenna deployment, as depicted in Fig. 1. Unlike conventional flexible-antenna systems, the length of the waveguide can be arbitrarily long, allowing the deployment of pinching antennas very close to the user to establish a strong line-of-sight (LoS) link. Furthermore, a PASS is inexpensive and easy to install, as its mechanism simply involves adding or removing dielectric materials.

Due to their unique properties, pinching-antenna-assisted communications have garnered increasing attention. The pioneering work in [5] analyzed the ergodic rate achieved

C. Ouyang and Z. Wang are with Queen Mary University of London, E1 4NS London, U.K. (e-mail: {c.ouyang, zhaolin.wang}@qmul.ac.uk).

Y. Liu is with the Department of Electrical and Electronic Engineering, The University of Hong Kong, Hong Kong (email: yuanwei@hku.hk).

Z. Ding is with Khalifa University, Abu Dhabi, UAE, and the University of Manchester, Manchester, M1 9BB, U.K. (e-mail: zhiguo.ding@ku.ac.ae).

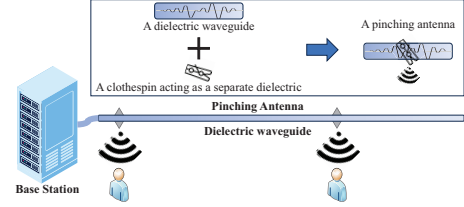


Fig. 1: Illustration of a PASS.

by employing pinching antennas to serve mobile users and theoretically characterized the performance gain of PASS over conventional fixed-position antenna systems. Building on this work, several algorithms have been proposed to optimize the activated positions of pinching antennas along the waveguide. These studies include optimization strategies for downlink single-user channels [6], downlink multiuser channels [7], and uplink multiuser channels [8].

Building on the contributions of these existing works, this article aims to provide further insights into the fundamental performance of PASS by analyzing the achievable array gain and addressing the following two questions regarding its behavior:

- 1) For fixed inter-antenna spacing, does the array gain *increase monotonically* with the number of antennas?
- 2) For a fixed antenna number, does the array gain *increase monotonically* as the inter-antenna spacing decreases?

Intuitively, the answers to these two questions are “yes”, as it seems natural to assume that using a larger number of antennas results in a higher array gain and that smaller inter-antenna spacing reduces path loss to the user. However, our analytical results presented in this work suggest that *the answers to both questions are actually “no”*.

The main contributions of this paper are summarized as follows: i) By fixing the inter-antenna spacing, we derive a closed-form upper bound on the array gain. Using this bound, we prove that the array gain does not always increase monotonically with the number of pinching antennas and that there exists an optimal antenna number to maximize the array gain. ii) By fixing the number of antennas, we analyze the relationship between the array gain and inter-antenna spacing while considering the effect of mutual coupling (MC) [9]. For the case of two antennas, we derive a closed-form approximation of the array gain. This analysis demonstrates that, due to MC, the array gain does not increase monotonically with decreasing inter-antenna spacing. iii) We provide numerical results to identify the optimal number of antennas and the optimal inter-antenna spacing. These results demonstrate the superiority of pinching antennas compared to conventional antennas.

II. SYSTEM MODEL

Consider a downlink communication system in which a base station (BS) serves a single-antenna user located at

$\mathbf{u} = [x_u, 0, 0]^T$, as illustrated in Fig. 2. For a theoretical exploration of the fundamental performance limits, we assume a basic free-space LoS propagation scenario.

A. Conventional-Antenna System

We first review the conventional antenna system, where the BS antenna is deployed at a fixed location. Without loss of generality, we assume that the BS antenna is positioned above the user at a height d , with its location denoted as $\psi_0 = [x_0, 0, d]^T$, where $x_0 = x_u$ is to be used in the simulation section. According to the spherical-wave channel model, the channel from the fixed antenna and the user is given by [10]:

$$h_0 = \frac{\eta^{\frac{1}{2}} e^{-j\frac{2\pi}{\lambda} \|\mathbf{u} - \psi_0\|}}{\|\mathbf{u} - \psi_0\|} = \frac{\eta^{\frac{1}{2}} e^{-j\frac{2\pi}{\lambda} \sqrt{(x_1 - x_0)^2 + d^2}}}{\sqrt{(x_1 - x_0)^2 + d^2}},$$

where $\eta = \frac{c^2}{16\pi^2 f_c^2}$, c denotes the speed of light, f_c is the carrier frequency, and λ is the wavelength in free space.

We have assumed that there is only one single antenna in the conventional antenna system, not only because it is expensive to add more antennas for the conventional case, but also because there is simply no such flexibility to the conventional case [5].

B. Pinching-Antenna System

For the PASS, we assume that N pinching antennas are activated on a waveguide to jointly serve the user, as depicted in Fig. 2. The waveguide is parallel to the x -axis at a height d . The channel vector between the pinching antennas and the user is given by

$$\mathbf{h} = [h_1; \dots; h_N] = \left[\frac{\eta^{\frac{1}{2}} e^{-j\frac{2\pi}{\lambda} \|\mathbf{u} - \psi_n\|}}{\|\mathbf{u} - \psi_n\|} \right]_{n=1}^N,$$

where $\psi_n = [x_n, 0, d]^T$ represents the location of the n th pinching antenna for $n = 1, \dots, N$.

Let $s \in \mathbb{C}$ denote the normalized signal transmitted through the waveguide. The received signal at the user is given by

$$y = \sqrt{\frac{P}{N}} \mathbf{h}^T \phi s + n, \quad (1)$$

where $n \sim \mathcal{CN}(0, \sigma^2)$ is Gaussian noise with variance σ^2 , P is the total transmit power, and $\phi = [e^{-j\phi_1}, \dots, e^{-j\phi_N}]^T$ represents the phase shifts of the signals received by the N pinching antennas. The phase shift of the signal received by the n th pinching antenna is $\phi_n = \frac{2\pi(x_n - x_u)}{\lambda_g}$, where $\lambda_g = \frac{\lambda}{n_{\text{neff}}}$ is the guided wavelength, and n_{neff} is the effective refractive index of the dielectric waveguide [11]. Assume that the transmit power is evenly distributed among the N active pinching antennas, which results in a per-antenna power of $\frac{P}{N}$. In the signal model shown in (1), the propagation loss within the waveguide is omitted, since in order to serve the user, it is expected that the antennas are placed closely and the propagation loss between the antennas is very small [7].

Therefore, the user's signal-to-noise ratio (SNR) for decoding s can be written as follows:

$$\gamma = \frac{P}{\sigma^2} \frac{|\mathbf{h}^T \phi|^2}{N}.$$

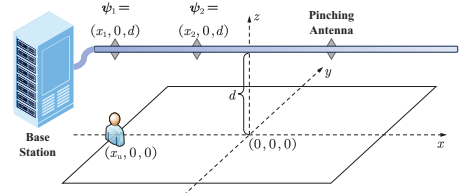


Fig. 2: Illustration of a PASS with a single waveguide and a single user.

The array gain achieved by the N antennas is given by

$$a = \frac{\gamma}{P/\sigma^2} = \frac{\eta}{N} \left| \sum_{n=1}^N \frac{e^{-j\frac{2\pi}{\lambda} \sqrt{d^2 + \Delta_n^2}} e^{-j\frac{2\pi \Delta_n}{\lambda_g}}}{\sqrt{d^2 + \Delta_n^2}} \right|^2,$$

where $\Delta_n \triangleq x_n - x_u$ for $n = 1, \dots, N$.

III. ANALYSIS OF THE ARRAY GAIN

A. Array Gain w.r.t. the Antenna Number

In this section, we address the first question by analyzing the relationship between the array gain and the number of antennas. For simplicity, we fix the inter-antenna spacing as $\frac{\lambda}{2}$ to eliminate MC effects between the pinching antennas [9]. Furthermore, we assume that the center of the array is placed directly above the user with N being an odd number, which yields $\{\Delta_n\} = \left\{ \frac{\lambda}{2} \tilde{n} \mid \tilde{n} = 0, \pm 1, \pm \tilde{N} \right\}$ with $\tilde{N} = \frac{N-1}{2}$. The resulting array gain can be expressed as follows:

$$a = \frac{\eta}{Nd^2} \left| \sum_{\tilde{n}=-\tilde{N}}^{\tilde{N}} \frac{e^{-j\frac{2\pi d}{\lambda} \sqrt{1 + \left(\frac{\lambda \tilde{n}}{2d}\right)^2}} e^{-j\frac{2\pi \lambda \tilde{n}}{\lambda_g} \frac{\lambda \tilde{n}}{2d}}}{\sqrt{1 + \left(\frac{\lambda \tilde{n}}{2d}\right)^2}} \right|^2. \quad (2)$$

We then denote $\varepsilon = \frac{\lambda}{d}$ and rewrite (2) as follows:

$$a = \frac{\eta}{Nd^2 \varepsilon^2} \left| \sum_{\tilde{n}=-\tilde{N}}^{\tilde{N}} \frac{e^{-j\frac{2\pi d}{\lambda} \sqrt{1 + \left(\frac{\tilde{n}\varepsilon}{2}\right)^2}} e^{-j\frac{2\pi d \varepsilon \tilde{n}}{\lambda_g} \frac{\varepsilon \tilde{n}}{2}}}{\sqrt{1 + \left(\frac{\tilde{n}\varepsilon}{2}\right)^2}} \varepsilon \right|^2.$$

Given that $\varepsilon = \frac{\lambda}{d} \ll 1$, we approximate the summation using the integral concept as follows:

$$a \approx \frac{\eta}{Nd^2 \varepsilon^2} \left| \int_{-\tilde{N}\varepsilon}^{\tilde{N}\varepsilon} \frac{e^{-j\frac{2\pi d}{\lambda} \left(\sqrt{1 + \frac{x^2}{4} + n_{\text{neff}} \frac{x}{2}} \right)}}{\sqrt{1 + \frac{x^2}{4}}} dx \right|^2. \quad (3)$$

Due to the complexity introduced by the term $e^{-j\frac{2\pi d}{\lambda} \left(\sqrt{1 + \frac{x^2}{4} + n_{\text{neff}} \frac{x}{2}} \right)}$, a closed-form solution for the integral in (3) is unavailable. Instead, we derive an upper bound on (2) and (3) as follows:

$$a \leq \frac{\eta}{Nd^2 \varepsilon^2} \left| \int_{-\tilde{N}\varepsilon}^{\tilde{N}\varepsilon} \frac{1}{\sqrt{1 + \frac{x^2}{4}}} dx \right|^2 \quad (4a)$$

$$= \frac{16\eta \left(\ln \left(\sqrt{1 + \frac{1}{4} \tilde{N}^2 \varepsilon^2} + \frac{\tilde{N}\varepsilon}{2} \right) \right)^2}{Nd^2 \varepsilon^2}. \quad (4b)$$

Building on this result, the following theorem is found.

Theorem 1. Given $\{\Delta_n\} = \left\{ \frac{\lambda}{2} \tilde{n} \mid \tilde{n} = 0, \pm 1, \pm \tilde{N} \right\}$, let $N \rightarrow \infty$. The asymptotic array gain achieved by the \tilde{N} pinching antennas satisfies $\lim_{N \rightarrow \infty} a = 0$.

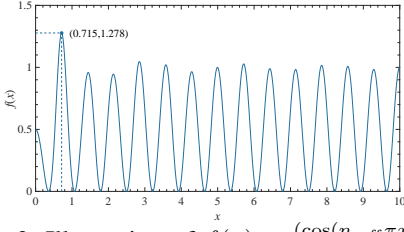


Fig. 3: Illustration of $f(x) = \frac{(\cos(n_{\text{neff}}\pi x))^2}{1+j_0(2\pi x)}$.

Proof: It holds that $\lim_{N \rightarrow \infty} \frac{(\ln(\sqrt{1+\frac{1}{4}N^2\varepsilon^2+\frac{N\varepsilon}{2}}))^2}{N} = 0$ for a given ε , which, together with (4) and the fact that $a \geq 0$ as well as the squeeze theorem, leads to $\lim_{N \rightarrow \infty} a = 0$. ■

The results in **Theorem 1** can be explained as follows. With N becomes infinite, $\frac{P}{N}$ becomes small, and the antennas with the majority power are too far away from the user, which makes the user receive negligible energy radiated from the pinching antennas.

Remark 1. *The above argument implies that, for the considered PASS, increasing the number of pinching antennas does not lead to a monotonic increase in the achievable array gain. Instead, there exists an optimal number of pinching antennas that maximizes the array gain.*

Unfortunately, due to the mathematical intractability of (2) and (3), finding a closed-form solution for the optimal number of pinching antennas is challenging. As a compromise, simulations are to be conducted in Section IV to gain further insights about the optimal number of pinching antennas.

B. Array Gain w.r.t. the Antenna Spacing

Having addressed the first question, we now focus on the second question regarding the relationship between the array gain and the inter-antenna spacing. Intuitively, once x_u , the x -coordinate of the user's location, is fixed, it is preferable to position all the antennas as close to x_u as possible, i.e., to set $x_n \approx x_u$ for $n = 1, \dots, N$. In this configuration, all antennas can provide strong LoS links to the user.

However, when the inter-antenna spacing is arbitrarily small, the effects of MC arise [9]. MC refers to the phenomenon where electromagnetic waves transmitted by one antenna are absorbed by its adjacent antennas, influencing their circuitry and altering the overall spatial channel. This effect can lead to significant performance degradation.

In this case, the spatial channel between the N pinching antennas and the user is described as follows [9, Eq. (105)]:

$$\mathbf{g} = [g_1; \dots; g_N] = \mathbf{C}^{-\frac{1}{2}} \mathbf{h}, \quad (5)$$

where $\mathbf{C} \in \mathbb{C}^{N \times N}$ represents the MC matrix. For simplicity, we assume the pinching antennas are evenly spaced with an inter-antenna spacing of Δ . In this case, \mathbf{C} is modeled as follows [9, Eq. (48)]:

$$\mathbf{C} = \begin{bmatrix} 1 & j_0(\frac{2\pi\Delta}{\lambda}) & \dots & j_0(\frac{2\pi\Delta(N-1)}{\lambda}) \\ j_0(\frac{2\pi\Delta}{\lambda}) & 1 & \dots & j_0(\frac{2\pi\Delta(N-2)}{\lambda}) \\ \vdots & \ddots & \ddots & \vdots \\ j_0(\frac{2\pi\Delta(N-1)}{\lambda}) & j_0(\frac{2\pi\Delta(N-2)}{\lambda}) & \dots & 1 \end{bmatrix}, \quad (6)$$

where $j_0(x) = \frac{\sin(x)}{x}$. When $\Delta = \frac{\lambda}{2}$, it follows that $\mathbf{C} = \mathbf{I}_N$, resulting in $\mathbf{g} = \mathbf{h}$, which indicates the absence of MC effects (as per Section III-A).

Based on (5), the array gain is given by

$$a = \frac{|\mathbf{g}^T \boldsymbol{\phi}|^2}{N} = \frac{|\mathbf{h}^T \mathbf{C}^{-\frac{1}{2}} \boldsymbol{\phi}|^2}{N}.$$

However, explicitly calculating $\mathbf{C}^{-\frac{1}{2}}$ is infeasible in general. As a compromise, we consider the case with two pinching antennas ($N = 2$) with $x_1 = x_u$ and $x_2 = x_u + \Delta$, which simplifies (6) to the following:

$$\begin{bmatrix} 1 & j_0(\frac{2\pi\Delta}{\lambda}) \\ j_0(\frac{2\pi\Delta}{\lambda}) & 1 \end{bmatrix} \triangleq \mathbf{C}_2. \quad (7)$$

Based on [12], the eigendecomposition of \mathbf{C}_2 is given by

$$\mathbf{C}_2 = \begin{bmatrix} \frac{-1}{\sqrt{2}} & \frac{-1}{\sqrt{2}} \\ \frac{-1}{\sqrt{2}} & \frac{1}{\sqrt{2}} \end{bmatrix} \begin{bmatrix} 1+j_0(\frac{2\pi\Delta}{\lambda}) & 0 \\ 0 & 1-j_0(\frac{2\pi\Delta}{\lambda}) \end{bmatrix} \begin{bmatrix} \frac{-1}{\sqrt{2}} & \frac{-1}{\sqrt{2}} \\ \frac{-1}{\sqrt{2}} & \frac{1}{\sqrt{2}} \end{bmatrix}.$$

It follows that

$$\mathbf{C}_2^{-\frac{1}{2}} = \begin{bmatrix} \frac{-1}{\sqrt{2}} & \frac{-1}{\sqrt{2}} \\ \frac{-1}{\sqrt{2}} & \frac{1}{\sqrt{2}} \end{bmatrix} \begin{bmatrix} \frac{1}{\sqrt{1+j_0(\frac{2\pi\Delta}{\lambda})}} & 0 \\ 0 & \frac{1}{\sqrt{1-j_0(\frac{2\pi\Delta}{\lambda})}} \end{bmatrix} \begin{bmatrix} \frac{-1}{\sqrt{2}} & \frac{-1}{\sqrt{2}} \\ \frac{-1}{\sqrt{2}} & \frac{1}{\sqrt{2}} \end{bmatrix}.$$

The resulting array gain is

$$\begin{aligned} a &= \frac{1}{2} |\mathbf{h}^T \mathbf{C}_2^{-\frac{1}{2}} \boldsymbol{\phi}|^2 = \frac{1}{2} |\boldsymbol{\phi}^T \mathbf{C}_2^{-\frac{1}{2}} \mathbf{h}|^2 \\ &= \frac{1}{8} \left| \frac{(h_1 + h_2)(1 + e^{-j\phi_2})}{\sqrt{1 + j_0(\frac{2\pi\Delta}{\lambda})}} + \frac{(h_1 - h_2)(1 - e^{-j\phi_2})}{\sqrt{1 - j_0(\frac{2\pi\Delta}{\lambda})}} \right|^2. \end{aligned} \quad (8a)$$

For simplicity, we assume $\Delta \ll d$, which implies $h_1 \approx h_2$. Consequently, (8) can be approximated as follows:

$$a \approx \frac{1}{8} \left| \frac{2h_1(1 + e^{-j\phi_2})}{\sqrt{1 + j_0(\frac{2\pi\Delta}{\lambda})}} \right|^2 = \frac{2\eta(\cos(\frac{2\pi\Delta}{2\lambda_g}))^2}{d^2(1 + j_0(\frac{2\pi\Delta}{\lambda}))} = \frac{2\eta}{d^2} f(m), \quad (9)$$

where $f(x) = \frac{(\cos(n_{\text{neff}}\pi x))^2}{1+j_0(2\pi x)}$, $\Delta = \lambda m$, and $\lambda_g = \frac{\lambda}{n_{\text{neff}}}$.

Due to the oscillations introduced by both $\cos(\cdot)$ and $j_0(\cdot)$, it is evident that (9) is not a monotonic function with respect to m or Δ . To gain further insights, Fig. 3 illustrates the values of $f(x)$ versus x for $n_{\text{neff}} = 1.4$ [5]. From the graph, $f(x)$ oscillates with x . Specifically, when x is small, $f(x)$ initially decreases before increasing again. This behavior indicates that the array gain initially declines and then rises as the inter-antenna spacing increases. This changing trend results from the combined effects of MC and wave propagation within the waveguide. The optimal value of x that maximizes $f(x)$ is found to be $x^* = 0.715$. Therefore, the optimal inter-antenna spacing for the considered system is given by $x^*\lambda = 0.715\lambda$, which answers the second question.

Remark 2. *For the considered PASS, reducing the inter-antenna spacing does not lead to a monotonic increase in the achievable array gain. Instead, there exists an optimal inter-antenna spacing for the pinching antennas that maximizes the array gain.*

IV. NUMERICAL RESULTS

In this section, we study the impact of the number of pinching antennas and their inter-antenna spacing on the array gain through computer simulations. Unless otherwise specified, the following parameter choices are used: $f_c = 28$ GHz, $d = 3$ m, $n_{\text{eff}} = 1.4$ [5], and $x_0 = x_u = -5$ m.

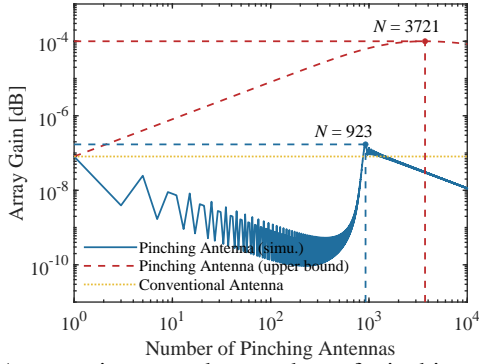


Fig. 4: Array gain w.r.t. the number of pinching antennas. $\{\Delta_n\} = \left\{ \frac{\lambda}{2} \tilde{n} \mid \tilde{n} = 0, \pm 1, \pm \frac{N-1}{2} \right\}$.

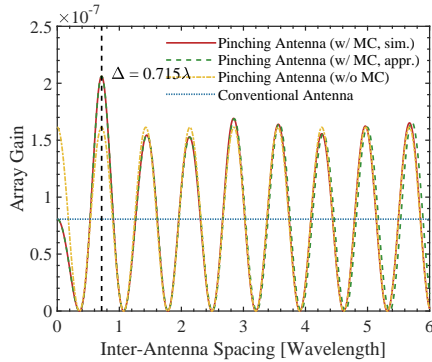


Fig. 5: Array gain w.r.t. the inter-antenna spacing. $N = 2$.

Fig. 4 illustrates the array gain as a function of the number of pinching antennas, N , with half-wavelength antenna spacing. For comparison, the upper bound on the array gain (as per (4b)) and the channel gain achieved by a conventional antenna are also presented. An important observation from Fig. 4 is that both the array gain achieved by the pinching antennas and its upper bound do not increase monotonically with N . Instead, there exists an optimal antenna number that maximizes the array gain, which verifies the conclusion drawn in **Remark 1**. As observed, the optimal number of pinching antennas is given by $N^* = 923$. Under our set-up, the resulting length of the required waveguide is $\frac{\lambda}{2} N^* = 4.94$ m. This is feasible for a waveguide deployed in indoor environments such as libraries or shopping malls. This further emphasizes the importance of optimizing the number of pinching antennas.

Furthermore, it is observed that the array gain achieved by the pinching antennas is smaller than that of the conventional fixed-position antennas across a wide range of antenna numbers. This is because, in the considered system, the positions of the pinching antennas are not optimized, potentially resulting in a lower array gain compared to the conventional setup. However, if the antenna number is set to its optimal value, $N^* = 923$, the PASS achieves a higher array gain than the conventional antenna. In our analysis, the positions of the pinching antennas are not optimized, which serves as a lower bound for practical systems. By further optimizing their positions, the PASS is able to achieve a higher array gain than the conventional system over a broad range of N . Initial results supporting this observation are available in [5]–[8].

Fig. 5 plots the array gain versus the inter-antenna spacing Δ when two pinching antennas are employed, as discussed in

Section III-B. The simulated array gain closely matches the approximated results (calculated by (9)) when Δ is small, and it nearly coincides with the results obtained without considering MC as Δ increases. This is because the approximation in (9) assumes $\Delta \ll d$, and the effect of MC becomes negligible when Δ is large. As shown in the graph, when MC is not considered, the optimal antenna spacing is $\Delta = 0$, indicating that positioning adjacent antennas as close as possible improves the array gain. This is effectively equivalent to increasing the effective aperture of a single antenna. However, when MC is taken into account, the array gain oscillates with Δ , and there exists an optimal inter-antenna spacing that maximizes the array gain. This supports the findings in **Remark 2**. Moreover, the optimal inter-antenna spacing observed in Fig. 5 aligns with the results shown in Fig. 3. Additionally, the maximum array gain achieved by the pinching antennas is larger than that of the conventional antenna.

V. CONCLUSION

This article has analyzed the array gain achieved by PASS. The carried-out analysis revealed that there exists an optimal number of pinching antennas and an optimal inter-antenna spacing that can maximize the array gain. These findings highlight the importance of optimizing the two parameters in practical PASS.

REFERENCES

- [1] K.-K. Wong, A. Shojaefard, K.-F. Tong, and Y. Zhang, "Fluid antenna systems," *IEEE Trans. Wireless Commun.*, vol. 20, no. 3, pp. 1950–1962, Mar. 2021.
- [2] L. Zhu, W. Ma, and R. Zhang, "Movable antennas for wireless communication: Opportunities and challenges," *IEEE Commun. Mag.*, vol. 62, no. 6, pp. 114–120, Jun. 2024.
- [3] "Pinching antenna," NTT DOCOMO, Inc., Tokyo, Japan, Tech. Rep., 2022. [Online]. Available: https://www.docomo.ne.jp/english/info/media_center/event/mwc21/pdf/06_MWC2021_06.pdf
- [4] A. Fukuda, H. Yamamoto, H. Okazaki, Y. Suzuki, and K. Kawai, "Pinching antenna: Using a dielectric waveguide as an antenna," *NTT DOCOMO Technical J.*, vol. 23, no. 3, pp. 5–12, Jan. 2022.
- [5] Z. Ding, R. Schober, and H. V. Poor, "Flexible-antenna systems: A pinching-antenna perspective," *arXiv:2412.02376*, 2024.
- [6] Y. Xu, Z. Ding, and G. K. Karagiannidis, "Rate maximization for downlink pinching-antenna systems," *IEEE Wireless Commun. Lett.*, Submitted, 2024. [Online]. Available: https://personalpages.manchester.ac.uk/staff/zhiguo.ding/pages/rate_max_pinching_antenna/
- [7] K. Wang, Z. Ding, and R. Schober, "Antenna activation for NOMA assisted pinching-antenna systems," *arXiv:2412.13969*, 2024.
- [8] S. A. Tegos, V. K. Papanikolaou, Z. Ding, and G. K. Karagiannidis, "Minimum data rate maximization for uplink pinching-antenna systems," *arXiv:2412.13892*, 2024.
- [9] M. T. Ivrlač and J. A. Nossek, "Toward a circuit theory of communication," *IEEE Trans. Circuits Syst. I, Regular Papers*, vol. 57, no. 7, pp. 1663–1683, Jul. 2010.
- [10] Y. Liu *et al.*, "Near-field communications: A tutorial review," *IEEE Open J. Commun. Soc.*, vol. 4, pp. 1999–2049, 2023.
- [11] D. M. Pozar, *Microwave Engineering: Theory and Techniques*. Hoboken, NJ, USA: Wiley, 2021.
- [12] C.-A. Deledalle, L. Denis, S. Tabti, and F. Tupin, "Closed-form expressions of the eigen decomposition of 2×2 and 3×3 Hermitian matrices," HAL, Lyon, France, Tech. Rep. hal-01501221, 2017. [Online]. Available: <https://hal.archives-ouvertes.fr/hal-01501221>